

Enhancement of nonlinear effects using photonic crystals

The quest for all-optical signal processing is generally deemed to be impractical because optical nonlinearities are usually weak. The emerging field of nonlinear photonic crystals seems destined to change this view dramatically. Theoretical considerations show that all-optical devices using photonic crystal designs promise to be smaller than the wavelength of light, and to operate with bandwidths that are very difficult to achieve electronically. When created in commonly used materials, these devices could operate at powers of only a few milliwatts. Moreover, if these designs are combined with materials and systems that support electromagnetically induced transparency, operation at single-photon power levels could be feasible.

MARIN SOLJAČIĆ* AND
J. D. JOANNOPOULOS

Physics Department, Massachusetts Institute of Technology,
Cambridge, Massachusetts 02139, USA.

*e-mail: marin@alum.mit.edu

Over the past several years, electronics has seen enormous advances in almost any application that has to do with information processing: following Moore's law, data density on a chip has doubled every 18 months. Although this trend is likely to continue for another decade, it clearly cannot last indefinitely: within the next two decades this growth is predicted to hit the insurmountable wall presented by the inherent physical limitations of electronics. Some of these limitations are already becoming manifest: as electronics in modern computers is forced to operate at ever-higher frequencies, power dissipation and consequent hardware heating are becoming a serious problem. The problem is greater still in nodes of optical telecommunication networks, where data must be processed electronically at even higher operational frequencies. Electronics is simply not suitable for operation at very high frequencies or bandwidths. In contrast, the optical domain is perfectly suited to operation at high frequencies. Consequently, it has been a trend in telecommunication networks to try to minimize the involvement of electronics in signal manipulation and to keep signals in the optical domain for as long as possible. Moreover, it is likely that even data transport between various electronic desktop computer parts will soon be done optically.

Unfortunately, optics too has inherent physical limitations that make signal manipulation in the optical domain difficult. There is a pressing need to find new physical mechanisms that would improve our ability to

manipulate light. Any possible solution has to be integrable: integration of many functions on the same chip leads to much lower production and operating costs. Furthermore, the constituent materials have to be compatible with other materials and devices on the same chip. In the quest for the optimal solution, photonic crystals^{1,2} have emerged as a unique and promising family of materials.

Photonic crystals (PhCs) are artificially created materials^{3–9} in which the index of refraction varies periodically between high-index regions and low-index regions. Such an environment presents to photons what the periodic atomic potential of a semiconductor presents to electrons. In particular, under the right conditions, a complete photonic bandgap opens: light for any frequency within the photonic bandgap is prohibited from propagation in any direction inside a PhC. Because of these similarities, PhCs are sometimes even called 'semiconductors for photons.' Just as semiconductors led to integration of electronics, PhCs are thought to be the most promising candidate to enable optical integration. They can be created from almost any material, so the material-compatibility requirement is automatically satisfied.

PhCs offer unprecedented opportunities for moulding the flow of light^{3,7,8}. Where the optical response remains linear, these opportunities have already been very successfully explored to create many elements (all with characteristic scales smaller than the wavelength of light) needed for passive control of light flow. To name a few examples, Noda *et al.* have demonstrated waveguides⁹, Fan *et al.* have proposed T-branches¹⁰, Chow *et al.* have produced sharp bends¹¹ and Fan *et al.* have designed channel-drops¹².

But for true all-optical signal processing, one needs a way of influencing light with light itself: one has to use optical nonlinearities. In optically nonlinear media, the

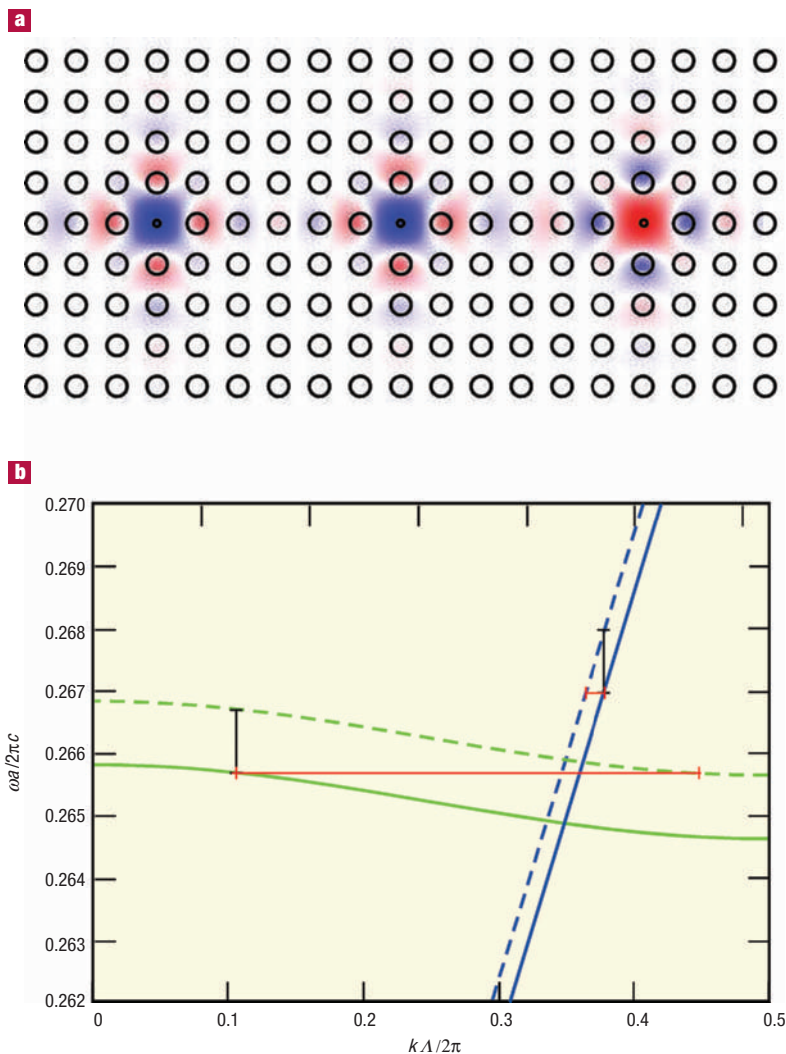


Figure 1 Numerical simulation of a coupled-cavities waveguide. **a**, A photonic crystal of high-index rods embedded in a low-index medium. The CCW is formed by decreasing the radius of every sixth rod in a line. The electric field of the guided mode is shown: blue denotes high-positive amplitude regions, whereas red denotes high-negative amplitude regions. The light tends to be localized close to the defects. **b**, The dispersion relation of the guided mode from **a** is shown by the solid green line. The guided mode inside a conventional high-index contrast waveguide is shown by the solid blue line. The same shift in ω (shown by the black lines: $\delta\omega = 0.001$) causes a much larger shift in k (the red lines) in the case of the CCW, owing to its slow group velocity. Here Λ is the separation of point defects (narrower rods), a the lattice constant, c the speed of light in vacuo and k the wavenumber.

index of refraction is modified by the presence of a light signal; this modification can be exploited to influence another light signal, thereby performing an all-optical signal processing operation. To operate efficiently at high bandwidths, one would prefer to use nonlinearities with ultra-fast (or nearly instantaneous) response and recovery times. Unfortunately, such nonlinearities are extraordinarily weak, thus requiring unacceptably huge operational powers, large interaction lengths or both. Two general approaches are usually taken to boost nonlinear effects. The first approach is material-oriented: one can try to find a material in which nonlinear effects are strongest. The second approach is

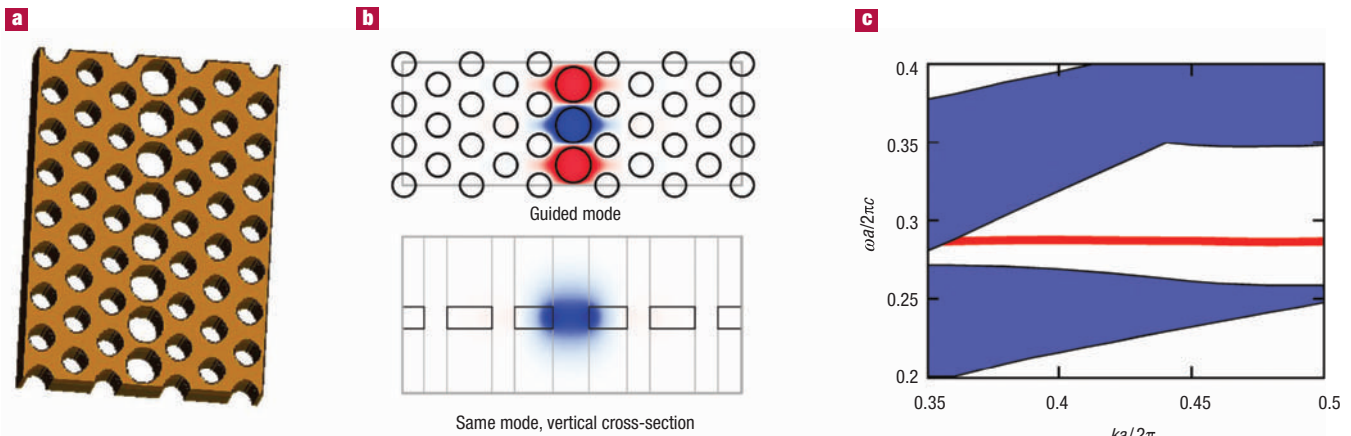
structural: one tries to find a structure whose geometrical properties optimize the nonlinear interaction of interest. Here again, PhCs offer unprecedented opportunities for structural enhancement of nonlinear effects. It is precisely these opportunities that are the topic of this review.

We focus on theoretical investigations; the PhC community is fortunate that the mathematical equations that describe PhC systems (nonlinear Maxwell's equations) are very suitable for numerical solutions. There are many powerful numerical tools available for modelling such systems, but one in particular deserves a special mention: finite-difference time domain (FDTD) calculations (for a review, see ref. 13) can simulate Maxwell's equations 'exactly' with no approximations apart from the discretization. Consequently, they are known to be able to reproduce experiments very closely, and are often referred to as 'numerical experiments'. They are the most widely used numerical tool in the PhC community, and most of the results presented here were obtained using such simulations.

The subsequent sections show how nonlinear PhCs^{14,15} allow the design of ultra-fast, all-optical signal processing devices that are miniature and suitable for integration. These devices could be made in many commonly used materials (for example, AlGaAs, or Si, or As₂Se₃), yet operate at powers of only a few milliwatts (thus being compatible with powers used in telecommunications today). We start by demonstrating how PhCs can be used to design waveguides in which signal propagation is orders of magnitude slower than the speed of light in air, and how nonlinear effects in such waveguides are greatly increased^{16–18}. We then look at how optimal bistable switching^{19–22} could be achieved in PhC microcavities. Finally, because PhCs impose minimal requirements on choice of materials, they are perfectly suited for taking advantage of both material and structural approaches for nonlinearity enhancement. For example, one could take materials that show the extraordinarily large nonlinearities enabled by electromagnetically induced transparency (EIT)²³ and combine them with PhC microcavities. One intriguing result might be to produce devices that display nonlinear effects at single-photon power levels. This possibility is discussed briefly in the section on EIT and in the concluding remarks.

SLOW-LIGHT WAVEGUIDES

Most commonly used optical switches and logical gates are based on interferometric designs. In an interferometric device, a signal is split into two waveguide-branches. To achieve a switching operation, one (or both) of these waveguides is manipulated with some stimuli, either external or internal, to control the relative phase difference between the two parts of the signal. At the output of the device, the two parts of the signal are made to interfere, so their relative phase determines the behaviour observed at the output. For example, constructive interference (relative phase $\Delta\phi = 0$) could mean a switch is ON (maximum output), whereas destructive interference (relative phase $\Delta\phi = \pi$) would then imply the switch is OFF (minimum output). As described below, the slow-light waveguides



created from PhCs improve the performance of such devices by a factor of $\sim(c/v_g)^2$ (ref. 18).

Imagine a waveguide in which the group velocity $v_g = d\omega/dk$ is much smaller than c (here, k is the wavenumber and ω is the angular frequency). Now consider using two such waveguides to create an interferometric switch. For clarity, the controlling stimulus is applied in only one of the two waveguide-branches. The influence of any ultra-fast stimulus is necessarily small: say it changes the index of refraction n of one of the materials from which the waveguide is made by a small amount δn . This problem can be analysed perturbatively¹⁸, to conclude that, to a good approximation, the resulting influence of δn is simply a parallel shift in the dispersion relation: $\omega(k) \rightarrow \omega(k) - \omega_s \delta n \sigma / n$, where ω_s is the signal's carrier frequency, and σ is the portion of the signal's energy contained in the material being affected. In a real physical setting, the incoming frequency is fixed, and the quantity that changes is k . The change in k determines the relative phase change between the two branches at the output of the device: $\Delta\phi = \Delta k(\omega_s)L$, where L is the waveguide length. The induced $\Delta k(\omega_s)$ can be calculated from the shift of the dispersion relation: $\Delta k(\omega_s) \approx -\omega_s \delta n \sigma / (n v_g)$. That is, the smaller the v_g of the waveguide, the shorter the waveguide length needed to induce a given phase shift.

As observed in the previous paragraph, using waveguides with low v_g saves a factor of $\sim c/v_g$ in the device length. Using such waveguides, however, also leads to savings in operational power. In the electro-optical case (when the index change $\delta n \propto |E|$ is induced by an external electrical field E), this is easy to see: the fact that one has to apply E in a volume that is c/v_g smaller means that one needs c/v_g less power to operate the device. In the all-optical Kerr case ($\delta n \propto |E|^2$, where E is the electric field of the controlling optical signal), the way to understand the power savings is as follows. Once the optical signal enters a slow-light waveguide, its length has to shrink (by a factor c/v_g) because the front end of the pulse 'sees' the slow- v_g region before the back end. The only way for it to shrink, yet conserve its energy, is for its $|E|^2$ to increase. Therefore, to induce a given δn , pulses that are a factor of c/v_g less energetic are needed. In fact, the savings in power and length can be traded for each other: if one is willing to keep the length

of a device fixed, one can afford to operate the device with $(c/v_g)^2$ less power, and vice versa. (Note that material absorption per unit length also increases by a factor (c/v_g) ; but because the true savings in device length (for a fixed power) are $(c/v_g)^2$, using slow-light waveguides is beneficial for improving a device's figure-of-merit with respect to material losses also.)

Unfortunately, in conventional waveguides (built from common materials) c/v_g is of the order of 1, so the discussion of the previous paragraph seems to be wishful thinking. PhCs change this picture: in PhCs, one can design v_g almost at will. In fact slow light occurs fairly commonly in PhCs; for example, waveguides with $v_g/c \approx 0.01$ have been implemented experimentally by Notomi *et al.*¹⁷ and by Inoue *et al.*²⁴. We focus our attention below on two examples of PhC slow- v_g waveguides.

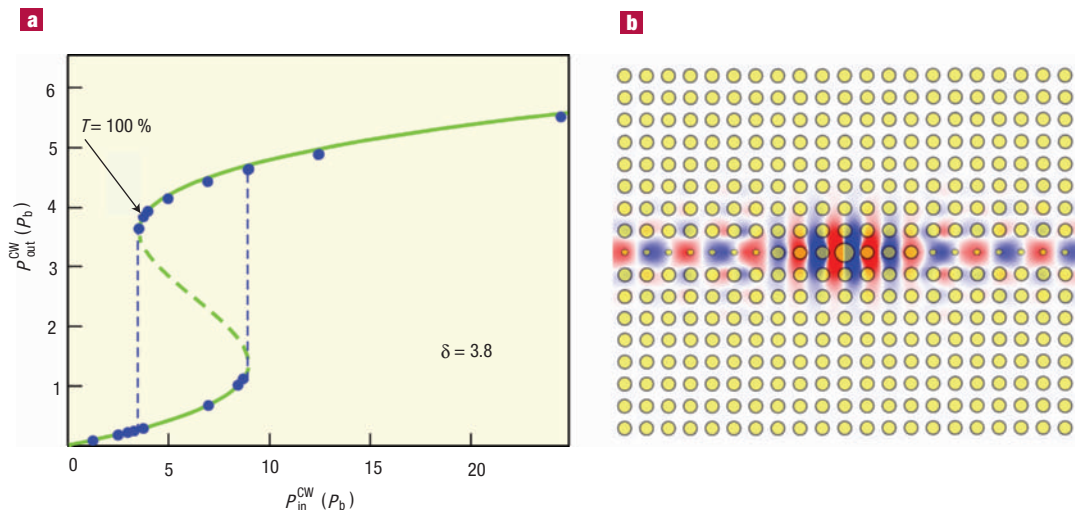
A PhC with a complete bandgap acts as a perfect mirror for frequencies within the bandgap. Imagine making a hole (point defect) deep inside such a PhC. Under proper conditions, this defect supports a resonant state: any light inside the defect will be trapped because the defect is the only place where light is allowed to exist. Imagine next creating a line defect by making a periodic array of such point defects (like in Fig. 1a), all mutually spaced some distance Λ apart, and placing some light inside one such point defect (here Λ is a few a , where a is the PhC lattice constant). The light can tunnel from the starting point defect to the neighbouring point defects, and from these to their neighbours. This way, light can propagate down this periodic line, and the line defect itself therefore acts as a waveguide. Because the process of transport is mediated through tunnelling, v_g of such a waveguide is slow: in fact, the further away the defects are, the slower v_g is. Such a waveguide is called a coupled-resonator oscillator waveguide (CROW) by Yariv *et al.*¹⁶, or a coupled-cavities waveguide (CCW) by Bayindir *et al.*²⁵. Enhancement of many nonlinear operations (including switching¹⁸ and wavelength conversion²⁶) has been described in such waveguides. An example of a CCW, together with the dispersion relation of its guided mode, is shown in Fig. 1.

CCWs have many attractive properties, but unfortunately (because $\Lambda \geq 2a$), they can be strictly implemented only in three-dimensional PhCs with complete photonic bandgaps. At the current state of

Figure 2 Slow-light waveguide made from a 2D-periodic photonic crystal slab.

a, Sketch of the structure; the distance between the holes would typically be a . **b**, A guided mode of this waveguide. **c**, The dispersion relation of the guided mode (red line in the panel); the group velocity of this mode is only $v_g = 0.016c$. Blue regions denote the modes that are not guided.

Figure 3 Optical bistability in a photonic crystal microcavity. **a.** $P_{\text{out}}^{\text{CW}}$ versus $P_{\text{in}}^{\text{CW}}$ for the photonic crystal bistable device shown in panel **b**. The blue dots are the results of numerical simulations. The green line is the analytical prediction; the middle (dashed) portion of the line is unstable and hence physically unobservable. **b.** A photonic crystal bistable device, here displaying electric field at 100% resonant linear transmission. The photonic crystal consists of high-index rods (yellow) in a low-index medium.



technology, such structures (for visible or near-infrared light) are still difficult to produce and work with. Until this problem is solved, one can resort to using line defects in two-dimensional-periodic PhC slabs²⁷ (like the one shown in Fig. 2a), which can be made in almost any semiconductor (or glass) in a single lithography step. These PhC slab line defects are periodic structures in which PhC effects provide waveguiding (along the line defect) in the plane of the slab, whereas high-index contrast provides waveguiding in the direction perpendicular to the plane. Such waveguides can be designed to support arbitrarily slow v_g modes; one such mode is shown in Fig. 2b and c.

At this point, a few words are in order to discuss the ultimate theoretical limits to enhancement of nonlinear effects using slow-light waveguides. As can be seen from Figs 1b and 2c, decreasing v_g comes at a price: the available bandwidth shrinks proportionally to v_g . Still, the performance characteristics offered by PhC waveguides can be impressive. Consider trying to make an all-optical switch for telecommunication wavelengths ($\lambda = 1.55 \mu\text{m}$) from AlGaAs (using its Kerr nonlinearity^{28,29}), with 100 GHz bandwidth (which would be very difficult to do with present-day electronics), operating at 10 mW power levels. It needs to be about 1.3 m long if produced from conventional high-index contrast waveguides, but only about 0.5 mm long when created with slow- v_g PhC waveguides. An added benefit of PhC waveguides (for example, those in Figs 1 and 2) is that (in contrast to most other slow-light waveguides) they can be nearly dispersionless, which is of enormous importance because it optimizes the available bandwidth¹⁸ and prevents signal distortion. Finally, PhC waveguides could potentially help with probably the most serious problem plaguing all high-index contrast waveguides: losses due to manufacturing imperfection (for example, wall surface roughness). Surrounding a waveguide with a PhC can eliminate scattering losses (as scattered waves are prohibited from propagating inside the PhC), whereas the reflections are unchanged (M. L. Povinelli, S. G. Johnson, E. Lidorikis, J. D. Joannopoulos and M. Soljačić, manuscript in preparation) This way the

total transmission down the waveguide can be significantly increased.

OPTICAL BISTABILITY IN PHOTONIC CRYSTAL MICROCAVITIES

Optical bistability is a fairly general phenomenon that occurs in many nonlinear systems with feedback³⁰. In such systems, the ratio of outgoing to incoming power (P_{out} versus P_{in}) can display a hysteresis loop (like the one shown in Fig. 3a), even when these systems are made from instantaneous-response materials: that is, these nonlinear systems have a memory of their past state despite the fact that none of the constituent materials have memory. In integrated electronics, flip-flops that show similar input–output relationships are used for pretty much any application: logic gates, memory, amplification, noise cleanup and so on. Not surprisingly, optical bistability has been successfully used in these same applications in the optical domain. Because of the extraordinary importance of its applications, enormous resources were devoted to the study of optical bistability in the 1980s (see ref. 31). Unfortunately, the systems developed during that period were not feasible for everyday use because of their size and operating powers, so research in the field slowed down. Here again, PhCs changed the picture, opening a new window of exciting opportunities for optical bistability. As discussed below for three different exemplary systems, using PhC microcavities one can observe bistability in systems that are of the order of λ^3 in size, made with commonly used materials, yet operating at only a few milliwatt power levels. Such systems were pioneered by Centeno and Felbacq¹⁹, Soljačić *et al.*²⁰, and Mingaleev and Kivshar²¹. Recently, Cowan and Young²² have presented a detailed analysis of such systems, including two-photon material absorption.

Consider a PhC system of nonlinear high-index rods, explored by Soljačić *et al.*²⁰, and shown in Fig. 3b, under continuous-wave (CW) excitations. It consists of a central optical cavity weakly and equally coupled (through tunnelling) to two channels (single-mode waveguides on the sides of the cavity). If we send light

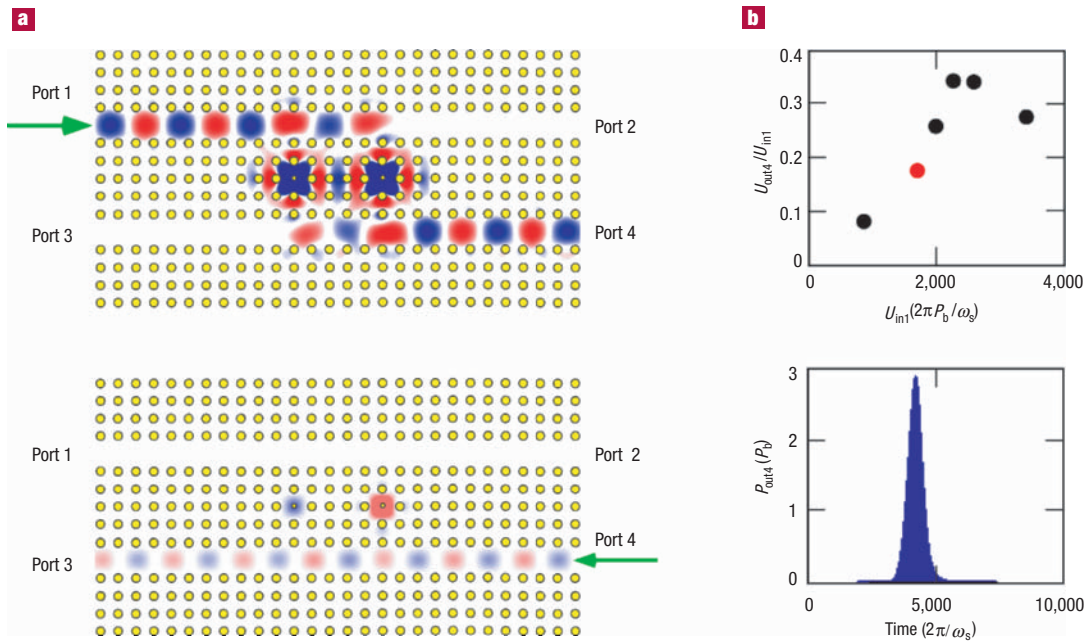


Figure 4 Numerical simulations of a two-defect photonic crystal device displaying optical bistability. **a**, As an example of the use of the device, the electric fields in the case when it performs optical isolation are shown. Top, a strong forward-propagating pulse. Bottom, a weak reflected backward-propagating pulse. We model the high index rods as having an instantaneous Kerr nonlinearity. **b**, Top, input–output relation for Gaussian signals of energy U_{in1} sent into port 1 (and observed at port 4) of the device from **a**; this transmission curve has large slope close to the red dot in the figure, which can be used for amplification. Bottom, a typical output signal observed at port 4 of the device: despite the extreme nonlinear effects, its initial Gaussian shape was not significantly distorted, which is of course important from the point of view of applications.

down one of these waveguides (input), the transmission to the other channel (output) in the linear regime has a Lorentzian shape (with width Γ) as a function of the carrier frequency ω_s , peaking at 100% for the resonant frequency ω_r of the cavity. The energy stored in the cavity is directly proportional to the outgoing power P_{out}^{CW} . Imagine next that the material inside the cavity is nonlinear, so the position of the resonant frequency depends on the energy stored in the cavity (which in turn depends on the detuning of the resonant frequency from the carrier frequency). Using perturbation theory in the small self-induced index change δn (ref. 20), one concludes that in the case of Kerr nonlinearity, the incoming power has a cubic-polynomial dependence on the energy inside the cavity (and thus the outgoing power), therefore explaining the shape shown in Fig. 3a

$$P_{in}^{CW} = P_{out}^{CW} \left[1 + \left(\frac{P_{out}^{CW}}{P_b} - \delta \right)^2 \right],$$

where $\delta = (\omega_r - \omega_s) / \Gamma$, and $P_b \propto \Gamma^2 / \kappa$ is the ‘characteristic power’ of this cavity: it sets the power scale at which bistable phenomena can be observed in a given cavity. (Here, κ is the nonlinear feedback parameter of the cavity²⁰: roughly, it is the inverse of the cavity’s modal volume, weighted by the local Kerr coefficient.)

The dependence of P_b on the cavity parameters Γ and κ can be easily understood^{32,33}. To obtain significant change of transmission through a cavity, its resonant frequency needs to be shifted by more than the cavity’s width Γ . This is where the first Γ factor in the expression $P_b \propto \Gamma^2 / \kappa$ comes from. The second factor of Γ comes from the field-enhancement effects inside the cavity: the smaller the Γ , the longer the light spends ‘bouncing around’ the cavity before escaping to the output, and as a result of this, the electric field E (and hence the self-induced δn) is much larger inside the cavity than in the waveguide outside the cavity. The fact that P_b should scale roughly as the modal volume can be understood as

follows: for a given energy stored inside the cavity (and hence a given P_{out}^{CW}), the induced $\delta n \propto |E|^2$ scales inversely with the modal volume). The fact that PhCs permit the creation of microcavities that have arbitrarily narrow resonances, at the same time as tiny modal volumes (less than $(\lambda/3)^3$ for the cavity in Fig. 3b), makes these systems optimal for optical bistability applications.

Their advantages lie not only in their extraordinary efficiency but also in the design flexibility they offer. Many different PhC cavity systems can be envisaged. Depending on their geometry, some of them are more suitable for certain applications than the others: for illustrative purposes, three such applications (optical isolation, optical transistor and all-optical switch) are presented below, in two different PhC microcavity systems.

Consider the PhC system shown in Fig. 4: it is left–right and up–down symmetric³⁴. It consists of two coupled cavities, weakly coupled to two single-mode waveguides. The two-cavity system supports one even $|e\rangle$ and one odd $|o\rangle$ state (with respect to the left–right symmetry). The system is designed so that $|e\rangle$ and $|o\rangle$ states are degenerate both in their resonant frequencies and in their lifetimes. Any waveguide excitation coming down ports 1 and/or 3 (for example, of the form e^{ikx}) can (because of its symmetry) couple only to a very particular superposition of the cavity states: $|e\rangle + i|o\rangle$. This state can in turn decay only into waveguide states of the form e^{ikx} ; it can decay only into ports 2 and/or 4. This is manifested physically in the fact that if ports 1 and/or 3 are used as the inputs of the device, there are never any reflections back into them; this applies both for the linear and the nonlinear regime³⁵. In fact, if port 1 is used as the input and port 4 as the output of the device, the input–output (linear and also nonlinear) relationship of this device is exactly the same as for the device of Fig. 3. However, in the device in Fig. 3,

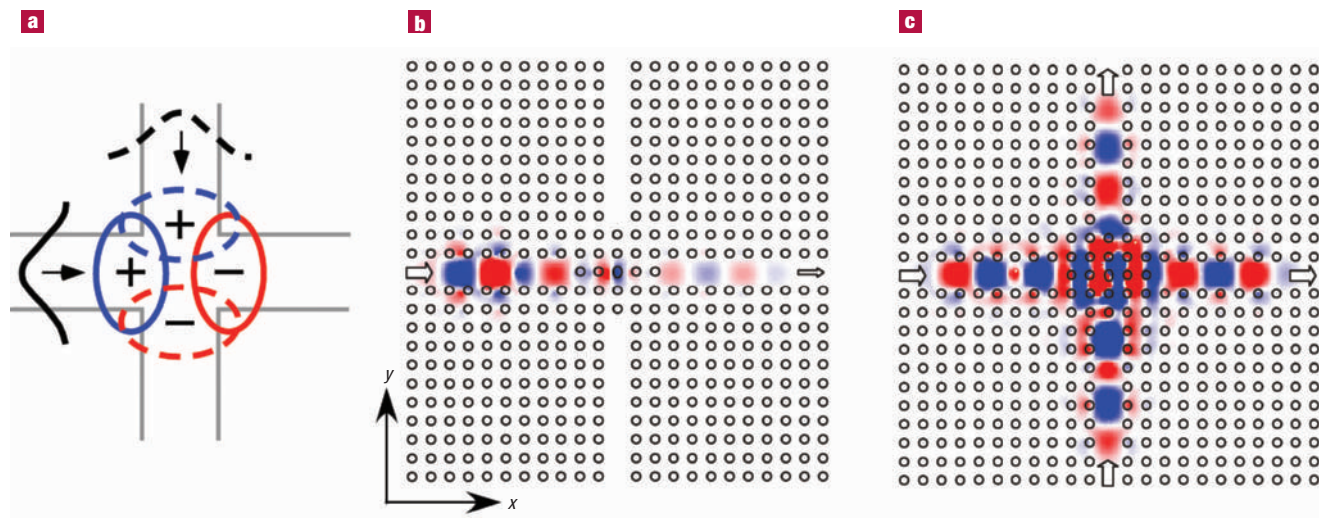


Figure 5 Photonic crystal optically bistable cross-switch. **a**, Symmetries of the involved modes prevent transfer of energy between signals propagating in x and y directions. If signals in both directions were tuned to be just below the onset of high-transmission regimes in their bistability hysteresis loops, then only the presence of both signals at the same time would trigger high transmission through the device. Thereby, the device acts as an all-optical logical AND gate, as shown in **b** and **c**. **b**, Signal present in a single direction only. **c**, Signals present in both directions.

whatever does not leave the output is reflected back to the input. In contrast, in the device in Fig. 4, whatever does not exit into port 4 is channelled into port 2.

The device in Fig. 4 can (among other things) be used for optical isolation. One of the biggest obstacles to achieving large-scale optics integration today is the lack of integrated optical isolators (active and nonlinear devices typically do not tolerate small reflections coming from other devices they are integrated with, so one has to have a way of discarding such reflections). The best approach involves breaking the time-reversal symmetry using magneto-optic materials. Unfortunately, even the optimal magneto-optic materials have only very weak magneto-optic effects (so the device size must be large), and such materials are notoriously difficult to integrate with other materials on the same chip. Until this problem is solved, one can use nonlinearities to implement optical isolation for many important applications^{36,37}. For example, the device of Fig. 4 can perform integrated-optics isolation when the strength of each logical (forward-propagating) signal in a particular waveguide is above the bistability threshold, and the reflected (backward-propagating) signals are weak. An example of such operation is shown in Fig. 4a. A strong forward-propagating signal (operating at a high-transmission point of the bistability curve) is nearly perfectly transferred from port 1 to port 4. However, when a weak reflected signal (operating at a low-transmission point of the bistability curve) enters port 4 of the device at a later time (coming from the neighbouring device down the line), it proceeds to port 3, from where it can be discarded. To make this scheme function properly, one has to be careful to place the neighbouring device at just the right distance so that these reflections would not coincide in time with any subsequent forward-propagating signals in the optical isolator.

The device from Fig. 4 can also be used as an all-optical transistor. Consider sending various energy (otherwise equal) gaussian signals of central carrier frequency ω_s into port 1 of the device (in a typical physical application, one is more likely to use gaussian

than continuous-wave signals). Imagine that $\delta = (\omega_r - \omega_s) / \Gamma$ is comparable to the one used in Fig. 3a, and that the signal's spectral width is comparable to the cavity's resonance width (albeit a bit smaller). As one might expect, the input–output relationship (top plot in Fig. 4b) looks like a 'smoothed-out' version of the lower hysteresis branch from Fig. 3a. Note that close to the red dot in Fig. 4b, the transmission curve has a large slope, which can be used for amplification. That is, imagine sending a train of signals (all of them represented by the red dot in Fig. 4b) into port 1 of the device, and in parallel with them, also sending much smaller gaussian signals into port 3, which would make the output slide up (or down) this large slope. The increment in the output observed at port 4 would then be a strongly amplified version of signals sent into port 3 (factors of 10 or 100 are easily achievable), so the device acts as an all-optical transistor.

As a final example, consider the device shown in Fig. 5: it has a single (central) cavity weakly coupled to four single-mode waveguides³⁸. It is up–down and left–right symmetric. The symmetries of all relevant modes of the device are illustrated in Fig. 5a. The cavity supports two dipole-type states: one of these states is odd with respect to the x axis and the other one is even. The mode propagating in the left or right waveguide (being even with respect to the x axis) can couple only to the cavity state that is even with respect to the x axis, and the mode propagating in the up or down waveguide can couple only to the other, odd, cavity state. Thus, no portion of the signal travelling along the x direction can be transferred into the y direction. Similarly, no portion of the signal travelling in the y direction can be transferred into the x direction. By making the central rod elliptical, one can break the degeneracy between the two states, so they have different resonant frequencies, ω_{rx} and ω_{ry} . The nonlinear behaviour of this device was studied by Yanik *et al.*³⁹. When light in only a single direction is present, the device behaves essentially the same as the device from Fig. 3 (for instance, the continuous-wave response for power present only in a single direction is exactly the same as that shown in

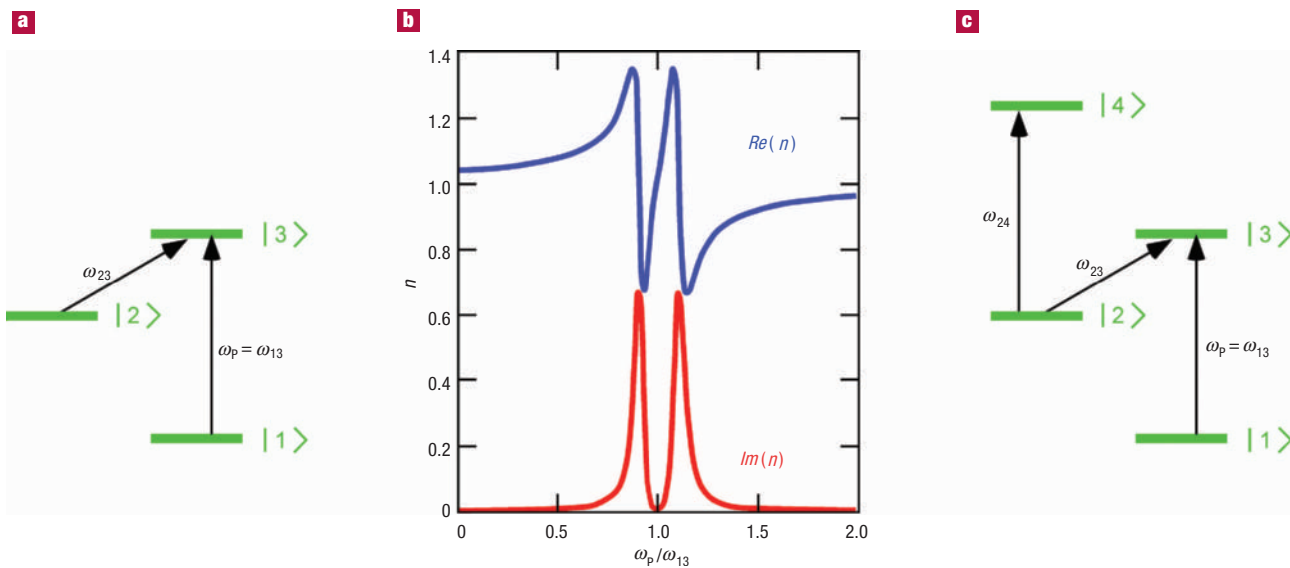


Fig. 3a). But when signals in both directions are present, one can use the signal in one direction to control the transmission in the other direction. Figure 5b and c shows how the device can be made to operate as an all-optical logical AND gate. Alternatively, the behaviour shown in Fig. 5b and c can be used for wavelength conversion: if one of the signals is just a periodic train of gaussian pulses at frequency ω_{sx} (propagating along the x direction), the information from the signal train at frequency ω_{sy} (propagating along the y direction) would be exactly transcribed into the signal train at frequency ω_{sx} .

All the devices described in this section are of order $O(\lambda^3)$ in size, so that, in principle, 10^6 of them could be placed on a surface of 1 mm^2 . In fact, devices of this type have already been demonstrated experimentally in the linear regime by Foresi *et al.*⁴⁰ and Yoshie *et al.*⁴¹. Closely related PhC microcavity lasers have also been produced by Painter *et al.*⁴². In the nonlinear regime, the operational power to observe bistability in PhC microcavities scales with the available bandwidth squared, but at 100 GHz bandwidth, and telecommunication wavelengths, one needs roughly 20–40 mW to operate such devices when made from AlGaAs (refs 20, 35, 39). If one is willing to operate at higher power levels, the bandwidth can be increased, but not indefinitely. The ultimate theoretical bandwidth is comparable to the maximum inducible change in the resonant frequency, which is in turn limited by the small size of the ultra-fast nonlinear effects.

TOWARDS SINGLE-PHOTON NONLINEARITIES

Imagine a two-level atomic system, with a ground state $|1\rangle$ and an excited state $|3\rangle$ (which is initially unpopulated). Probe light, whose frequency ω_p is very close to the resonance ω_{13} for the $|1\rangle \rightarrow |3\rangle$ transition, experiences huge absorption when propagating through such a material. But imagine at the same time shining a continuous-wave light of frequency ω_{23} which is exactly on resonance with the $|2\rangle \rightarrow |3\rangle$ transition (where $|2\rangle$ is some other, initially unpopulated, level),

as shown in Fig. 6a. Through the quantum interference phenomenon EIT²³, the absorption of ω_p is hugely suppressed; suppression by over 30 orders of magnitude has been observed by Hau *et al.*⁴³ in such systems. Because of ω_{23} , the absorption peak $Im\{n\}$ acquires a narrow dip (thus suppressing absorption), and $Re\{n\}$ acquires an additional ‘wiggle’ as seen in Fig. 6b. Note that close to the resonant frequency ω_{13} , $n(\omega_p)$ has a very large slope, meaning that v_g is very small; $v_g/c < 10^{-7}$ have been measured⁴³. Finally, consider also coupling level $|2\rangle$ resonantly (through frequency ω_{24}) with some fourth level $|4\rangle$ (as in Fig. 6c), causing a strong Stark shift of level $|2\rangle$. This nonlinear interaction becomes greatly amplified by the tiny group velocity, so the sensitivity of the induced $\delta n(\omega_p)$ to small intensities in ω_{24} is enormous. Kerr nonlinearities 12 orders of magnitude larger than in AlGaAs have been observed this way⁴³, so EIT materials are the most nonlinear materials in nature.

It is thus intriguing to consider combining the unparalleled nonlinear properties of EIT materials with the superb structural enhancement of nonlinear effects offered by PhC microcavities to produce an all-optical switch that can be operated at extraordinarily low power levels. (Detailed analysis of this system will be presented elsewhere; M. Soljačić, E. Lidorikis, J. D. Joannopoulos and L. Hau, manuscript in preparation.) For example, one could start with a PhC microcavity similar to the one shown in Fig. 3b, and dope it with a single EIT atom. Alternatively, one could use solid-state EIT materials⁴⁴, or else a single-gas-atom PhC microcavity⁴⁵. All of these systems would behave basically in the same manner. A density of one atom per modal volume ($\sim(\lambda/3)^3$) turns out to be roughly the same as the atom density in the EIT experiment of ref. 43, so roughly the same Kerr nonlinearity would apply. Next, an analysis similar to the one used earlier to estimate the operational powers of optically bistable devices (but this time with 10^{12} times stronger nonlinearities) leads to the conclusion that the ω_p transmission can be switched on and off with a mere 10^{-14} W or so of power in the signal ω_{24} . That is, having

Figure 6 Basics of EIT. **a**, Level schematic for a typical EIT system which suppresses absorption at ω_p . **b**, A typical example of $n(\omega_p)$ for an EIT system. **c**, Applying only a weak field at frequency ω_{24} in an EIT system with the schematic levels shown here can cause a large change in $n(\omega_p)$.

$O(10^{-9}) \omega_{24}$ photons in the cavity can switch the device from being ON into being OFF. Of course, at these minuscule powers, one would be totally swamped by temperature and even quantum fluctuations, so this is definitely not a desirable regime for operation. Nevertheless, this simple result indicates that systems of this kind are natural candidates for exploration of nonlinearities at single-photon power levels as studied by Werner and Imamoglu⁴⁶.

One can clearly afford to be a bit wasteful regarding the power specifications of the above device in order to improve some other characteristic of interest. For example, the system has a very narrow available bandwidth⁴⁷, because of the narrow width of the useful EIT window from Fig. 6b. The size of this window can be widened by increasing the intensity of the field at frequency ω_{23} . As this window becomes wider, however, v_g also increases, thereby lowering the nonlinear effects. Nevertheless, our preliminary calculations (M. Soljačić, E. Lidorikis, J. D. Joannopoulos and L. Hau, manuscript in preparation) indicate that using this approach one should be able to obtain an operational bandwidth of $O(1 \text{ GHz})$, while still operating at single-photon power levels. Such a device could therefore potentially have important applications for all-optical quantum information processing.

A PROMISING FUTURE

PhCs have opened many new windows of opportunity in the field of nonlinear optics. The earliest work on nonlinear PhCs dates from the 1970s, continuing into the 1990s, and focused naturally on one dimension^{48–61}. Since then, interest in nonlinear PhCs has grown rapidly. We refer the reader to two excellent overviews of this entire field by Slusher and Eggleton¹⁵, and by Bowden and Zheltikov⁶². Of particular note are the recent successes in two-dimensional nonlinear PhCs by Broderick *et al.*⁶³, who demonstrated second-harmonic generation using multiple reciprocal lattice vectors, and by Fleischer *et al.*⁶⁴, who demonstrated for the first time the existence of spatial solitons in 2D photonic lattices.

Nonlinear PhCs are likely to have the most significant technological impact in signal processing. For a long time, there was a widespread belief in the optics community that all-optical signal processing was not feasible because ultra-fast nonlinear effects were too small. Over the past few years, theoretical breakthroughs in nonlinear PhCs have changed all that. PhC designs seem to offer the feasibility of any kind of signal processing, with bandwidths that are very difficult to implement electronically, at power levels of only a few milliwatts. One might think that these power levels are not sufficiently low if one considers arrays of many such devices together. But in contrast to electronic signal processing, such low-energy signals are not even consumed during operations (apart for the small material losses), so they can be recycled without causing any heating of the device. Combining EIT with PhCs, even single-photon operational power levels might be achievable. The devices described above are fully compatible with large-scale integration: the material constraints are minimal, their ports are single-mode waveguides,

and they are tiny in size. In fact, 3D PhCs offer a promise of true 3D large-scale optical logic integration (rather than the planar integration used in electronics today). Around the world, the race is on to observe these and other promising performance characteristics experimentally. In the next few years, nonlinear PhCs are bound to be an exciting field.

References

- Yablonovitch, E. Inhibited spontaneous emission in solid-state physics and electronics. *Phys. Rev. Lett.* **58**, 2059–2062 (1987).
- John, S. Strong localization of photons in certain disordered dielectric superlattices. *Phys. Rev. Lett.* **58**, 2486–2489 (1987).
- Joannopoulos, J. D., Meade, R. D. & Winn, J. N. *Photonic Crystals: Molding the Flow of Light* (Princeton Univ. Press, Princeton, 1995).
- Lin, S. Y. *et al.* A three-dimensional photonic crystal operating at infrared wavelengths. *Nature* **394**, 251–253 (1998).
- Campbell, M., Sharp, D. N., Harrison, M. T., Denning, R. G. & Turberfield, A. J. Fabrication of photonic crystals for the visible spectrum by holographic lithography. *Nature* **404**, 53–56 (2000).
- Vlasov, Yu. A., Bo, X.-Z., Sturm, J. C. & Norris, D. J. On-chip natural assembly of silicon photonic bandgap crystals. *Nature* **414**, 289–293 (2001).
- Sakoda, K. *Optical Properties of Photonic Crystals* (Springer, Berlin, 2001).
- Johnson, S. G. & Joannopoulos, J. D. *Photonic Crystals: The Road from Theory to Practice* (Kluwer, Norwell, 2002).
- Noda, S., Tomoda, K., Yamamoto, N. & Chutinan, A. Full three-dimensional photonic bandgap crystals at near-infrared wavelengths. *Science* **289**, 604–606 (2000).
- Fan, S., Johnson, S. G., Joannopoulos, J. D., Manolatu, C. & Haus, H. A. Waveguide branches in photonic crystals. *J. Opt. Soc. Am. B* **18**, 162–165 (2001).
- Chow, E., Lin, S. Y., Wendt, J. R., Johnson, S. G. & Joannopoulos, J. D. Quantitative analysis of bending efficiency in photonic-crystal waveguide bends at $\lambda = 1.55 \mu\text{m}$ wavelengths. *Opt. Lett.* **26**, 286–288 (2001).
- Fan, S. *et al.* Theoretical analysis of channel drop tunneling processes. *Phys. Rev. B* **59**, 15882–15892 (1999).
- Taflove, A. *Computational Electrodynamics: The Finite-Difference Time-Domain Method* (Artech House, Norwood, 1995).
- Bhat, N. A. R. & Sipe, J. E. Optical pulse propagation in nonlinear photonic crystals. *Phys. Rev. E* **64**, 056604 (2001).
- Slusher, R. E. & Eggleton, B. J. *Nonlinear Photonic Crystals* (Springer, Berlin, 2003).
- Yariv, A., Xu, Y., Lee, R. K. & Scherer, A. Coupled-resonator optical waveguide: a proposal and analysis. *Opt. Lett.* **24**, 711–713 (1999).
- Notomi, M. *et al.* Extremely large group-velocity dispersion of line-defect waveguides in photonic crystal slabs. *Phys. Rev. Lett.* **87**, 253902 (2001).
- Soljačić, M. *et al.* Photonic-crystal slow-light enhancement of nonlinear phase sensitivity. *J. Opt. Soc. Am. B* **19**, 2052–2059 (2002).
- Centeno, E. & Felbacq, D. Optical bistability in finite-size nonlinear bidimensional photonic crystals doped by a microcavity. *Phys. Rev. B* **62**, R7683–R7686 (2000).
- Soljačić, M., Ibanescu, M., Johnson, S. G., Fink, Y. & Joannopoulos, J. D. Optimal bistable switching in nonlinear photonic crystals. *Phys. Rev. E* **66**, 055601R (2002).
- Mingaleev, S. F. & Kivshar, Y. S. Nonlinear transmission and light localization in photonic-crystal waveguides. *J. Opt. Soc. Am. B* **19**, 2241–2249 (2002).
- Cowan, A. R. & Young, J. F. Optical bistability involving photonic crystal microcavities and Fano line shapes. *Phys. Rev. E* **68**, 046606 (2003).
- Harris, S. E. Electromagnetically induced transparency. *Phys. Today* **50**, 36–42 (July 1997).
- Inoue, K. *et al.* Observation of small group velocity in two-dimensional AlGaAs-based photonic crystal slabs. *Phys. Rev. B* **65**, 121308R (2002).
- Bayindir, M., Temelkuran, B. & Ozbay, E. Tight-binding description of the coupled defect modes in three-dimensional photonic crystals. *Phys. Rev. Lett.* **84**, 2140–2143 (2000).
- Mookherjee, S. & Yariv, A. Second-harmonic generation with pulses in a coupled-resonator optical waveguide. *Phys. Rev. E* **65**, 026607 (2002).
- Johnson, S. G., Villeneuve, P. R., Fan, S. & Joannopoulos, J. D. Linear waveguides in photonic-crystal slabs. *Phys. Rev. B* **62**, 8212–8222 (2000).
- Islam, M. N. *et al.* Nonlinear spectroscopy near half-gap in bulk and quantum well GaAs/AlGaAs waveguides. *J. Appl. Phys.* **71**, 1927–1935 (1992).
- Villeneuve, A., Yang, C. C., Stegeman, G. I., Lin, C. & Lin, H. Nonlinear refractive-index and two-photon-absorption near half the band gap in AlGaAs. *Appl. Phys. Lett.* **62**, 2465–2467 (1993).

30. Saleh, B. E. A. & Teich, M. C. *Fundamentals of Photonics* (Wiley, New York, 1991).
31. Gibbs, H. M. *Optical Bistability: Controlling Light with Light* (Academic, New York, 1985).
32. Heebner, J. E. & Boyd, R. Enhanced all-optical switching by use of a nonlinear fiber ring resonator. *Opt. Lett.* **24**, 847–849 (1999).
33. Yariv, A. Critical coupling and its control in optical waveguide-ring resonator systems. *IEEE Photon. Technol. Lett.* **14**, 483–485 (2002).
34. Fan, S., Villeneuve, P. R., Joannopoulos, J. D. & Haus, H. A. Channel drop tunneling through localized states. *Phys. Rev. Lett.* **80**, 960–963 (1998).
35. Soljačić, M., Luo, C., Joannopoulos, J. D. & Fan, S. Nonlinear photonic crystal microdevices for optical integration. *Opt. Lett.* **28**, 637–639 (2003).
36. Scalora, M., Dowling, J. P., Bloemer, M. J. & Bowden, C. M. The photonic band edge optical diode. *J. Appl. Phys.* **76**, 2023–2026 (1994).
37. Gallo, K., Assanto, G., Parameswaran, K. R. & Fejer, M. M. All-optical diode in a periodically poled lithium niobate waveguide. *Appl. Phys. Lett.* **79**, 314–316 (2001).
38. Johnson, S. G. *et al.* Elimination of crosstalk in waveguide intersections. *Opt. Lett.* **23**, 1855–1857 (1998).
39. Yanik, M. F., Fan, S., Soljačić, M. & Joannopoulos, J. D. All-optical transistor action with bistable switching in a photonic crystal cross-waveguide geometry. *Opt. Lett.* **28**, 2506–2508 (2003).
40. Foresi, J. S. *et al.* Photonic-bandgap microcavities in optical waveguides. *Nature* **390**, 143–145 (1997).
41. Yoshie, T., Vuckovic, J., Scherer, A., Chen, H. & Deppe, D. High quality two-dimensional photonic crystal slab cavities. *Appl. Phys. Lett.* **79**, 4289–4291 (2001).
42. Painter, O. *et al.* Two-dimensional photonic band-gap defect mode laser. *Science* **284**, 1819–1821 (1999).
43. Hau, L. V., Harris, S. E., Dutton, Z. & Behroozi, C. H. Light speed reduction to 17 metres per second in an ultracold atomic gas. *Nature* **397**, 594–598 (1999).
44. Turukhin, A. V. *et al.* observation of ultraslow and stored light pulses in a solid. *Phys. Rev. Lett.* **88**, 023602 (2002).
45. Vuckovic, J., Loncar, M., Mabuchi, H. & Scherer, A. Design of photonic crystal microcavities for cavity QED. *Phys. Rev. E* **65**, 016608 (2001).
46. Werner, M. J. & Imamoglu, A. Photon-photon interactions in cavity electromagnetically induced transparency. *Phys. Rev. A* **61**, 011801R (1999).
47. Lukin, M. D., Fleischhauer, M., Scully, M. O. & Velichansky, V. L. Intracavity electromagnetically induced transparency. *Opt. Lett.* **23**, 295–297 (1998).
48. Winful, H. G., Marburger, J. H. & Garmire, E. Theory of bistability in nonlinear distributed feedback structures. *Appl. Phys. Lett.* **35**, 379–381 (1979).
49. Chen, W. & Mills, D. L. Gap solitons and the nonlinear optical response of superlattices. *Phys. Rev. Lett.* **58**, 160–163 (1987).
50. Mecozzi, A., Trillo, S. & Wabnitz, S. Spatial instabilities, all-optical limiting, and thresholding in nonlinear distributed-feedback devices. *Opt. Lett.* **12**, 1008–1010 (1987).
51. Christodoulides, D. N. & Joseph, R. I. Slow Bragg solitons in nonlinear periodic structures. *Phys. Rev. Lett.* **62**, 1746–1749 (1989).
52. de Sterke, C. M. & Sipe, J. E. Extensions and generalizations of an envelope-function approach for the electro-dynamics of nonlinear periodic structures. *Phys. Rev. A* **39**, 5163–5178 (1989).
53. Russell, P. S. J. Bloch wave analysis of dispersion and pulse propagation in pure distributed feedback structures. *J. Mod. Opt.* **38**, 1599–1619 (1991).
54. Agrawal, G. P. & Dutta, N. K. *Semiconductor Lasers* 2nd edn (Van Nostrand Reinhold, New York, 1993).
55. Lidorikis, E., Busch, K., Li, Q., Chan, C. T. & Soukoulis, C. M. Optical nonlinear response of a single nonlinear dielectric layer sandwiched between two linear dielectric structures. *Phys. Rev. B* **56**, 15090–15099 (1997).
56. Emplit, P., Haelterman, M., Kashyap, R. & Lathouwer, M. D. Fiber Bragg grating for optical dark soliton generation. *IEEE Photon. Technol. Lett.* **9**, 1122–1124 (1997).
57. Peschel, T., Peschel, U., Lederer, F. & Malomed, B. A. Solitary waves in Bragg gratings with a quadratic nonlinearity. *Phys. Rev. E* **55**, 4730–4739 (1997).
58. Fiore, A., Berger, V., Rosencher, E., Bravetti, P. & Nagle, J. Phase matching using an isotropic nonlinear optical material. *Nature* **391**, 463–466 (1998).
59. Eisenberg, H. S., Silberberg, Y., Morandotti, R., Boyd, A. R. & Aitchison, J. S. Discrete spatial optical solitons in waveguide arrays. *Phys. Rev. Lett.* **81**, 3383–3386 (1998).
60. Clausen, C. B. & Torner, L. Spatial switching of quadratic solitons in engineered quasi-phase-matched structures. *Opt. Lett.* **24**, 7–9 (1999).
61. Sibilcia, C. *et al.* Electromagnetic properties of periodic and quasi-periodic one-dimensional, metallo-dielectric photonic band gap structures. *J. Opt. A—Pure Appl. Opt.* **1**, 490–494 (1999).
62. Bowden, C. M. & Zheltikov, A. M. *J. Opt. Soc. Am.* **19** (Feature issue No. 9) *Nonlinear Optics of Photonic Crystals* (September 2002).
63. Broderick, N. G. R., Ross, G. W., Offerhaus, H. L., Richardson, D. J. & Hanna, D. C. Hexagonally poled lithium niobate: a two-dimensional nonlinear photonic crystal. *Phys. Rev. Lett.* **84**, 4345–4348 (2000).
64. Fleischer, J. W. *et al.* Observation of two-dimensional discrete solitons in optically induced nonlinear photonic lattices. *Nature* **422**, 147–150 (2003).

Acknowledgements

Marin Soljačić would like to dedicate this article to the memory of his mother, Prof. Dr Marija Soljačić (1940–2003), for her enormous love and support.